THEORETICAL AND APPLIED MECHANICS
Volume 50 (2023) Issue 2, 133–144 DOI: https://doi.org/10.2298/TAM231012010S

WMLES OF FLOWS AROUND SMALL-SCALE PROPELLERS – ESTIMATING AERODYNAMIC PERFORMANCE AND WAKE VISUALIZATION

Jelena Svorcan

Abstract. Wall-modeled large-eddy simulation (WMLES) is an advanced mathematical model for turbulent flows which solves for the low-pass filtered numerical solution. A subgrid-scale (SGS) model is used to account for the effects of unresolved small-scale turbulent structures on the resolved scales (i.e. for the dissipation of the smaller scales), while the flow behavior near the walls is modeled by wall functions (thus reducing the requirements for mesh fineness/quality). This paper investigates the possibilities of applying WMLES in the estimation of aerodynamic performance of small-scale propellers, as well as in the analysis of the wake forming downstream. Induced flows around two propellers designed for unmanned air vehicles (approximately 25 cm and 75 cm in diameter) in hover are considered unsteady and turbulent (incompressible or compressible, respectively). Difficulties in computing such flows mainly originate from the relatively low values of Reynolds numbers (several tens to several hundreds of thousands) when transition and other flow phenomena may be present. The choice of the employed numerical model is substantiated by comparisons of resulting numerical with available experimental data. Whereas global quantities, such as thrust and power (coefficients), can be predicted with satisfactory accuracy (up-to several percents), distinguishing the predominant flow features remains challenging (and requires additional computational effort). Here, wakes forming aft of the propeller rotors are visualized and analyzed. These two benchmark examples provide useful guidelines for further numerical and experimental studies of small-scale propellers.

1. Introduction

Even though rotating lifting surfaces have been developed and investigated for centuries, scientific interest in them is not waning due to the expansion of modern unmanned air vehicles (UAVs) and future urban aircraft that are (and will be) equipped with numerous rotors. These small-scale propellers are usually made of composite and/or plastic materials, and should comply with the following design requirements: highly efficient aerodynamic performance, reliability in various operating regimes, decreased noise, compatibility with the accompanying electric

2020 *Mathematics Subject Classification:* 76-10; 76F65.
Key words and phrases: UAV propeller, WMLES, wake, aerodynamic performance, hover.

motor (having matching characteristics), economic production and maintenance. To achieve best performance, generated flow fields should be adequately modeled, understood in detail, and manipulated accordingly. However, this is often impeded by the strong interaction between the blades and the shed vortices, transition to turbulence in the vicinity of the blade leading edge (at smooth composite blades the flow usually starts off as laminar), and the fact that there is a lack of adequate models that can accurately represent these highly unsteady and complex flows at relatively coarse computational meshes. Some examples of numerical and experimental investigations of small-scale rotors are available in [1–9].

To provide sufficiently accurate and usable results, contemporary numerical simulations require refined meshes, miniscule time scales and advanced approach to modeling/partially resolving turbulence [2, 5, 9]. Still, owing to the acceptable balance between computational cost and global accuracy, the most employed computational fluid dynamics (CFD) approach is solving the unsteady Reynolds-averaged Navier-Stokes (URANS) equations [1,3,4,6,8]. The emerging alternative is a more complex and computationally expensive numerical model, wall-modeled large-eddy simulation (WMLES) [9–11], capable of resolving a large portion of turbulent motion, that becomes computationally acceptable when employed on moderately refined meshes. Therefore, this study is a continuation of previous research [8, 9] of low-to-medium Reynolds number (Re) flows around two different small-scale propeller rotors in hover, now resolved by WMLES, with a particular focus on generated wake (shed vortices). The ability to accurately predict the thrust T and power P of the two hovering small-scale propellers (approximately 25 cm and 75 cm in diameter) at different angular velocities (and consequently Re) is investigated, and some recommendations are provided.

2. Basics and comparison of numerical models URANS and WMLES for propeller flows

Propeller analysis usually starts with hover, the most basic flight condition, difficult to simulate due to: zero inflow across outer boundaries; induced velocity field around the rotor; uneven load distribution along the blades; transition to turbulence; wake/tip vortex formation, expansion, development, interaction with the blades and final breakdown; aeroelasticity of the blades; mutual effects of multiple rotors; possible effects of surrounding channels; aerodynamic noise, etc. To deal with some of these issues URANS or WMLES (that resolve at least a portion of the turbulence spectrum) are usually employed.

The chosen numerical approach/model dictates the way the geometry and computational mesh are generated. Most often, the rotating portion of the computational domain is shaped like a revolution body, whereas blade leading edge, root and tip segments are modeled with care since they directly influence transition to turbulence, profile drag and wake formation, particularly at low-to-medium Re. Trip (near the leading edge) is often introduced to enforce transition end ensure dominantly turbulent flow along the blade (that most often happens in real applications due to the high sensitivity of transitional flows to outer disturbances).

Computational grids are most often hybrid unstructured (comprising hexahedral or other prismatic, preferably less skewed cells), refined in the wall/blade vicinity because of the sudden changes of flow quantities inside the boundary layer (BL) (different wall functions are employed to avoid drastic increases in mesh size), and aft of the rotor to better capture the tip vortices and the developing wake. It is experimentally confirmed that the shed wake is very complex, comprising both primary (helicoidal) and secondary structures (rings around the main helicoids) that evolve and break down [12]. Adaptive mesh refinement may be employed to capture the wake shape, but many rotor rotations are needed, in turn causing numerical dissipation and instabilities [13]. For that reason, a combination of different modeling approaches and experimental validation is still very much desired and necessary.

The primary advantage of RANS approach is computational simplicity. By assuming a quasi-steady flow field where inertial terms from the rotation are added to the equations, it is possible to obtain a reasonable preliminary estimation of averaged aerodynamic loads. By simulating the rotor rotation and actually moving a part of the mesh (closely encompassing the blades) enables the consideration of transient effects (hence URANS). On the other hand, large-eddy simulation (LES), a scale-resolving turbulence modeling approach requiring small spatial and temporal scales, is generally capable of providing higher levels of accuracy than (U)RANS (e.g. in separated flows, or when jets or noise issues are important). However, its computational cost increases dramatically at higher Re (and thinning of BL and pertaining viscous sublayer). WMLES reduces the computational cost of wall-resolved (WR)LES by resolving larger-scale turbulent motion, while SGS motion (appearing in the wall vicinity, in the inner region of turbulent boundary layers) is considered more isotropic and can be modeled/specially treated [10, 11]. Numerous wall models have been proposed and tested.

An excellent review of WMLES basics is provided in [10, 11]. The governing equations for LES are derived by applying spatial filtering (to a filter width, usually comparable to mesh size) to the Navier-Stokes equations. The resulting stress tensor then consists of viscous and subgrid-scale terms, and an adequate expression for the SGS tensor should be provided. Another issue, for less refined meshes near boundaries, is the wall treatment. Within BLs, the size of energetic eddies is comparable with viscous length, whereas in the outer zone, BL thickness is the relevant length scale. Since their ratio is related to wall shear stress, initially, the values of local wall shear stress were prescribed along boundaries. Later, more involved wall-stress models, based on both ordinary and partial differential equations were developed.

Another possibility are hybrid LES/RANS approaches (an example in [5]), where RANS is applied within BLs (or a specific near-wall zone), and LES in the remainder of the computational domain.

Even though WMLES has been applied on a variety of problems, the greatest number of studies based on WMLES consider flows within simple domains. That is why it is very interesting to test this approach on small-scale propellers where

numerous flow phenomena appear. Here, two different geometries and commercial codes/suites are employed and contrasted.

3. Problem description

The geometry of small-scale propeller blades can be defined by the spanwise distributions of airfoil (thickness and curvature), pitch (i.e. twist) and chord. Nowadays, due to the use of modern materials and novel manufacturing technologies, these distributions are usually non-linear, resulting in rather complex and curved shapes. Here, two different rotors (approximately 25 cm and 75 cm in diameter) are considered, Fig. 1. Their detailed geometric descriptions may be found in [7, 8].

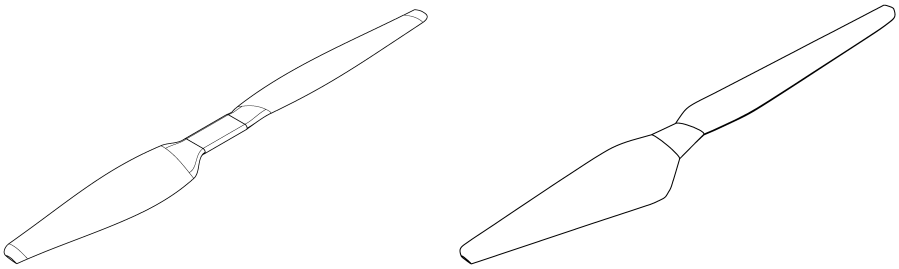

FIGURE 1. Illustrations of the two propellers: approx. 75 cm in diameter (left), and approx. 25 cm in diameter (right).

In comparison to standard helicopter airfoils, some of whose issues are considered in [14], the airfoils used here are specifically designed for small-scale propellers.

3.1. Computational set-up for the 75 cm propeller. Two starting geometric models were investigated – isolated and non-isolated propeller (with the included test stand and measuring equipment as illustrated in Fig. 2 (left)). In both cases, smooth walls are assumed, and blade surface triangulation is of sufficient quality (resolution) to accurately represent the leading and trailing edge details (such as curvatures and small edge lengths) and assure that neither the initially laminar flow at the leading edge nor the transition to turbulence is artificially affected by the geometric representation.

Computational meshes are generated by building Voronoi diagrams and smoothing the point distribution with Lloyd iteration in the mesh generator Stitch also developed by Cascade Technologies, Inc. Additionally, computational meshes incorporate layers of thin prismatic cells along the blade walls using boundary layer (so-called stranded) meshes to better capture the steep velocity gradient inside the boundary layer. To assure that grid features do not affect the final results, a mesh convergence study was conducted, where both medium and fine meshes performed very similarly (differences in converged thrust and power are less than 1%). A view of the generated fine mesh around the non-isolated rotor is shown in Fig. 2. It contains approximately 27 million control volumes (Mcvs), while the medium mesh generated around the isolated rotor numbers approximately 13 Mcvs.

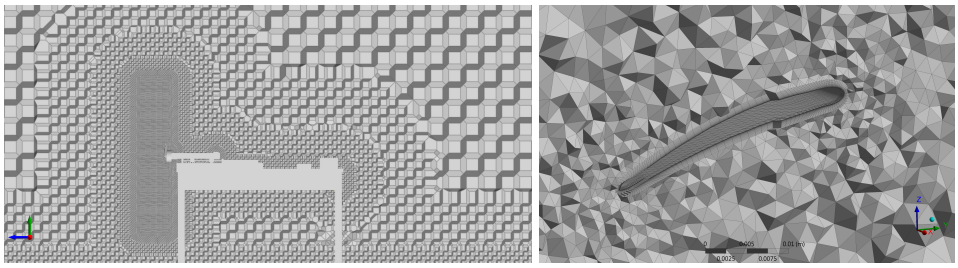

FIGURE 2. Details of the generated meshes around the: 75 cm rotor (left), and 25 cm rotor (right).

Flow fields around the 75 cm propeller rotating at several different angular velocities are computed by the GPU-accelerated finite-volume-based compressible flow solver charLES developed by Cascade Technologies, Inc. that solves the spatially filtered conservation equations governing the flow with the addition of the ideal gas equation of state. In this compressible formulation, the effects of rotation are incorporated by actually moving (i.e., rotating) the inner portion of the mesh in every time step, that is, by using the arbitrary Lagrangian-Eulerian (ALE) moving mesh approach. The two zones are separated by the interface boundary where Voronoi diagrams along the interface surface are recomputed/regenerated anew in every time step. The SGS stresses resulting from the filtering process are modeled by the Vreman model [15], whereas a no-penetration stress-based algebraic equilibrium wall model [16] is applied along the rotating propeller walls as well as the stationary surrounding objects and the floor. Characteristic boundary conditions with zero-velocity conditions are applied on all the remaining outer surfaces. The flow is initialized from the rest. Standard values of air properties are assumed.

The time step on the fine mesh and nominal angular velocity corresponds to an angular increment of 0.0025° (keeping CFL below 5 throughout the domain due to the explicit formulation). Computations are performed until achieving the convergence of aerodynamic force and moment (averaged per rotation), which was usually 25 rotations in total; where flow statistics were collected during the last five rotations. The simulations in this paper were performed using Chapman at the Center for Turbulence Research, composed of eight AMD Radeon Instinct MI50 GPUs.

3.2. Computational set-up for the 25 cm propeller. Similar steps to the previously mentioned were followed in the case of the smaller propeller. Here, only isolated geometry was investigated. To simulate the rotation, the computational domain was split into two zones where the inner zone, encompassing the propeller (radius 0.2 m, length 0.4 m), rotates. The outer zone is 10 times larger in every direction. Boundaries of the domain include inlet, outlet, blade walls and an interface between the two zones.

Mesh numbering nearly 8 Mcvs is generated, where special attention was paid to the airfoil contour and leading and trailing edge (a detail is provided in Fig. 2),

as well as blade tips and interface surface. Again, the inflation option was used, i.e. 25 layers of thin prismatic cells encompass the rotating walls. They grow by the factor of 1.1, with the resulting dimensionless wall distance $y^+ < 5$ along the blades. As will be shown later in the text, this mesh should be additionally refined to approach $y^+ \approx 1$.

Computations are performed using the finite-volume-based flow solver ANSYS FLUENT. Apart from using two different solvers, and considering this flow as incompressible (to reduce the computational cost), most of the remaining flow assumptions are comparable. Again, WMLES with algebraic wall function is employed. Standard air properties are assumed, zero gauge pressure is assumed along the outer boundaries, and the inner zone rotates with the assigned angular velocity. As numerical dissipation can be a major issue with LES, higher-order, low-dissipation schemes are employed, even for temporal discretization. Since implicit formulation is used in this case, time-step corresponds to a 1° angular increment (resulting in 360 per revolution, with 20 iterations per time-step). Again, computations are performed until achieving quasi-convergence of global aerodynamic properties, usually 20–25 revolutions.

4. Results and discussion

4.1. Global aerodynamic performance. Distributions of aerodynamic loads along rotating blades determine the two fundamental global aerodynamic quantifiers of propellers: generated thrust T at a required torque Q/power P, that are necessary for subsequent analyses (such as flight dynamics, stability and control, structural reliability) and dictate the success of the complete system/aircraft. Unfortunately, there are numerous challenges to their accurate determination, both experimental and computational. On one hand, blade dimensions are small and real geometric features deviate from the modeled, airfoils designed for low Re are somewhat specific, insufficiently tested and highly sensitive to outer disturbances, whilst high angular velocities require the use of sophisticated measuring equipment. Even when great care is taken, error bars appear quite wide, particularly when torque is investigated [7]. Still, it is possible to make comparisons between available experimental [7, 8] and obtained numerical data, and draw some useful conclusions. As illustrated in Fig. 3, a very satisfactory correspondence of thrust forces can be achieved even at Re spanning from approximately 80 to 300 thousand (based on the representative cross-section located at 3/4 blade length). For both rotors, the slightly bigger (diameter 75 cm) on the left, and the smaller (diameter 25 cm) on the right, differences between numerical and measured values remain within the error bars. The (beneficial) effects of experimental stand on aerodynamic performance (increased thrust) and the wake are also visible. A surprisingly good correlation between measured and computed power is achieved in all cases (Fig. 4).

4.2. Wake quantification and visualization. The computed instantaneous vortical structures shedding from the blade tips of the two propellers (delineated by Q-criterion isosurface and colored by Mach number or velocity where blue corresponds to zero and red to maximal values), and forming the wake are illustrated

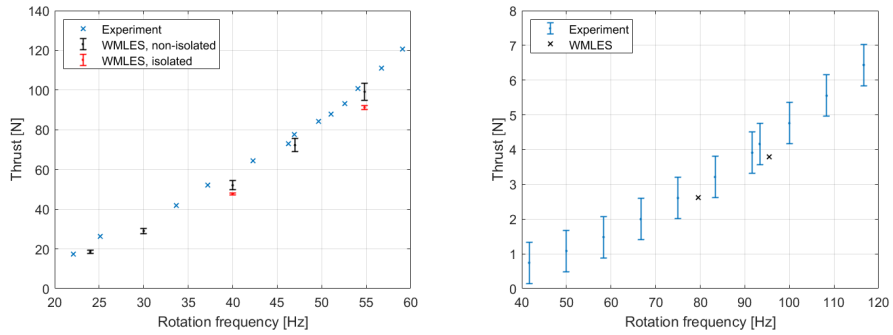

FIGURE 3. Computed vs. measured thrust force: 75 cm propeller (left), 25 cm propeller (right).

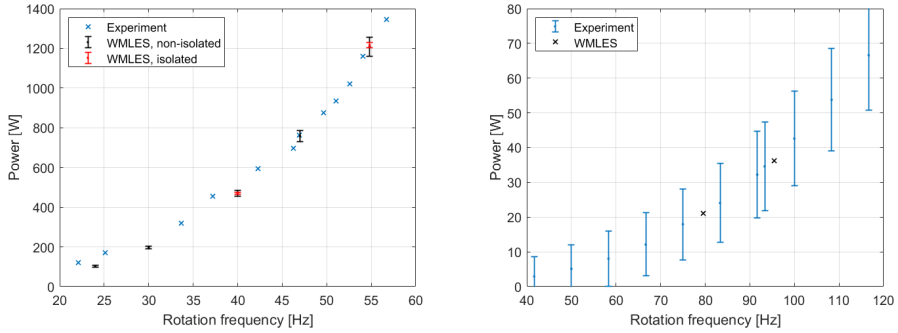

FIGURE 4. Computed vs. measured power: 75 cm propeller (left), 25 cm propeller (right).

in Figs. 5 and 6. It is immediately apparent that more representative flow visualizations are obtained on the more refined mesh generated around the 75 cm propeller and by the charLES flow solver. Apart from the main vortex system comprising the two helical wakes originating from the blade tips, smaller secondary structures forming around it are also visible. Whereas these secondary structures are partially the consequence of numerical artifacts, their existence has also been experimentally confirmed [12]. The mutual interaction of the blades and the wakes as well as the vortices shedding from the blade root sections seem well captured. As demonstrated in [9], the existence of the test stand and equipment downstream of the rotor can be responsible for the redistribution of aerodynamic loads in comparison to the performance of a clean, isolated propeller. It can also be concluded that the other mesh (containing approximately 8 Mcvs) may not be sufficient to accurately capture all the complexities of the wake that should comprise both primary helicoidal and secondary vortices (forming around the primary structures). However, primary structures as well as blade/wake interaction seem partly apprehended. Furthermore, the contribution of the root segments to the wake formation is well depicted.

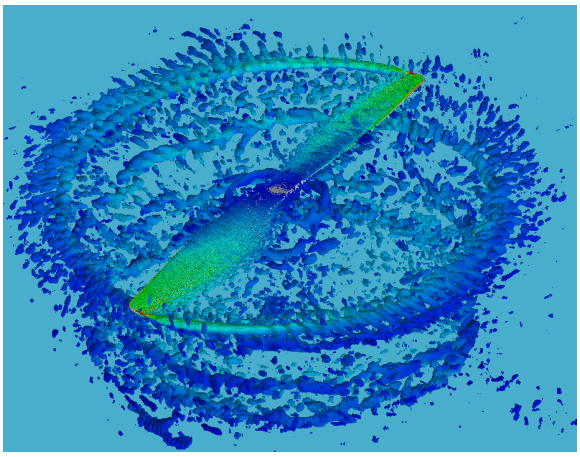

FIGURE 5. Wake behind the isolated 75 cm propeller computed by charLES.

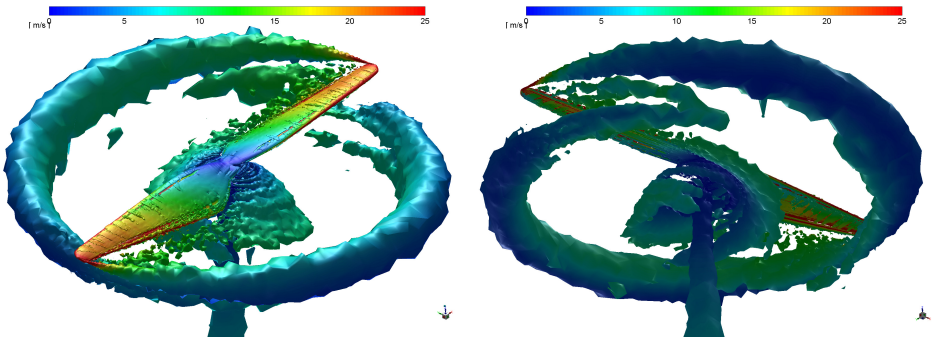

FIGURE 6. Wake behind the 25 cm propeller computed by ANSYS FLUENT.

It is also interesting to analyze the averaged velocity fields and visualize the wake structure and evolution in the aft cross-sections. Figure 7 shows the computed velocity contours in the 75 cm rotor plane and several equally spaced downstream planes. Several distinct zones can be identified. In the rotor plane, the two vortices shedding from the blade tips are dominant, whereas the root zone (of slightly reversed flow) is also notable. These two initial vortices, forming the wake, even out as they move away from the rotating blades (the main source of disturbance) and, initially, the wake becomes more contracted (resulting in the increase of induced axial velocity). Ultimately, sufficiently far away from the rotor, the wake will completely dissipate.

Similar representations, but from a different perspective (in the longitudinal plane), can be made for the smaller 25 cm propeller, see Fig. 8. The wake shape is clearly separated from the remaining domain where velocity is nearly zero (which demonstrates why quasi 1-D models, although simple, are still very much used and

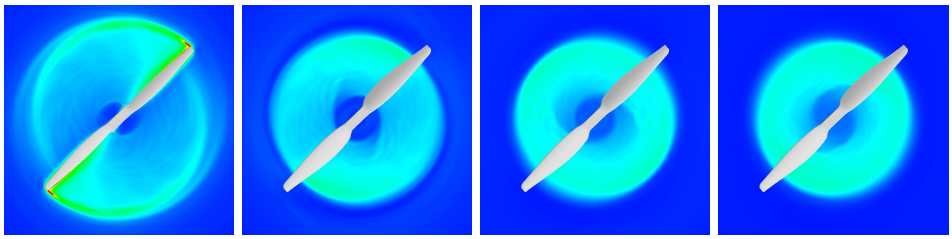

FIGURE 7. Wake behind the 75 cm propeller computed by charLES and represented by averaged velocity fields.

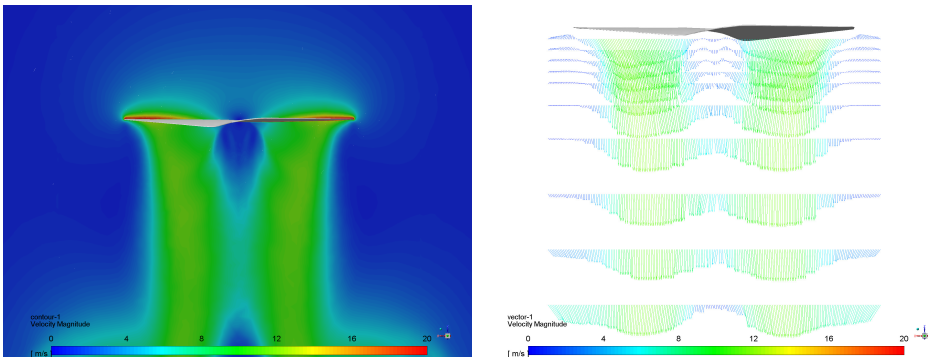

FIGURE 8. Wake around the 25 cm propeller computed by ANSYS FLUENT and represented by averaged velocity fields.

provide satisfactory initial estimations). The wake is initially disjointed, comprising several (here two) main vortices that originate from the blades, and that merge later downstream. They will again dissolve as the complete induced velocity field dissipates into the surrounding steady air.

The wake can additionally be quantified (and not merely qualitatively presented) by the downstream axial and tangential velocity profiles, see Fig. 9 and [17]. Looking at the axial velocity profiles, several different segments can be discerned. Within the root portion, we can even observe slightly reversed flow directly below the rotor. This is followed by the steep, nearly linear increase of the axial velocity (up to the approximate relative coordinate $x/R = 0.3$) which then slowly transforms to another nearly constant function along the operational part of the blade ($0.3 < x/R < 0.8$). As we approach the blade tips (and even sooner, as the wake contracts), the axial velocity drops to zero. Again, the weakening of the wake and induced velocity field in the far downstream planes is apparent (axial velocity profile flattens). Whereas these results directly depend on the blade geometry and adopted airfoil, they also provide a useful representation of the wake evolution (initial growth followed by dissipation). On the other hand, tangential velocity profiles seem more scattered. Immediately below the rotor, the values are the highest (but still significantly smaller than axial velocities), and they drop very soon. Whereas

there are a lot of occurrences in the flow in the intermediate planes, the tangential velocity distribution approaches that of the Rankine vortex further downstream.

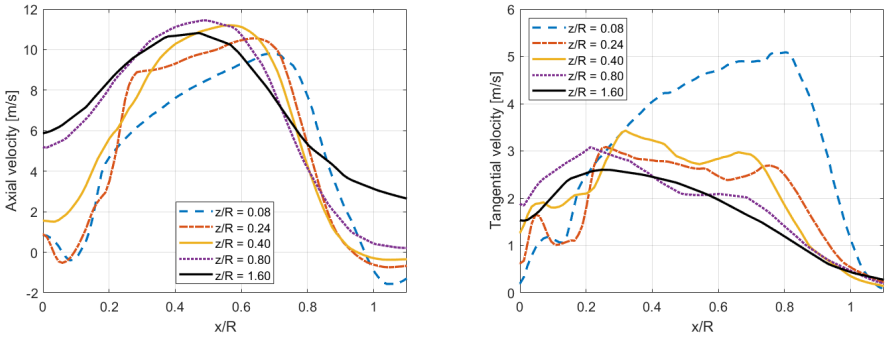

FIGURE 9. Axial (left) and tangential (right) velocity profiles behind the 25 cm propeller computed by ANSYS FLUENT.

5. Conclusions

The paper addresses some of the issues present in the contemporary simulations of the flows around propeller rotors. Some basic characteristics of small-scale structures are outlined, in terms of geometry (increased curvature), (stringent) mesh requirements, operating conditions (usual operation in *filthier* flows) and flow physics (small-scale structures usually involve both laminar and turbulent flows, as well as the computationally very delicate transitional flows).

The most employed CFD techniques are URANS and WMLES. Generally, URANS still present a good compromise between accuracy and computational cost, and are excellent for initial and optimization studies (estimated thrust error can be below 10%). When more in-depth analysis is necessary, it is recommended to opt for some of the scale-resolving models, such as WMLES. However, the potential accuracy increase will be highly dependent on the quality of both the starting geometry and the generated mesh (fine resolution is a prerequisite, and prismatic layers around the walls corresponding to BL appear very helpful), as well as the flow assumptions and the employed numerical schemes. Ideally, experiment and WMLES should be used and combined whenever possible.

Acknowledgments. J. S. conducted a part of this research during a Fulbright Fellowship at Stanford University, Center for Turbulence Research from November 2021 till July 2022. This research work is also supported by the Ministry of Science, Technological Development and Innovation of the Republic of Serbia through contract no. 451-03-47/2023-01/200105 from February 3rd, 2023.

References

1. M. Carreño Ruiz, M. Scanavino, D. D'Ambrosio, G. Guglieri, A. Vilardi, *Experimental and numerical analysis of hovering multicopter performance in low-Reynolds number conditions*, Aerosp. Sci. Technol. **128** (2022), 107777.

2. C. Wang, P. Li, C. Guo, L. Wang, S. Sun, *Numerical research on the instabilities of CLT propeller wake*, Ocean Eng. **243** (2022), 110305.
3. T. Zhang, G. N. Barakos, *High-fidelity numerical analysis and optimisation of ducted propeller aerodynamics and acoustics*, Aerosp. Sci. Technol. **113** (2021), 106708.
4. A. Garofano-Soldado, P. J. Sanchez-Cuevas, G. Heredia, A. Ollero, *Numerical-experimental evaluation and modelling of aerodynamic ground effect for small-scale tilted propellers at low Reynolds numbers*, Aerosp. Sci. Technol. **126** (2022), 107625.
5. J. C. Nathanael, C.-H. J. Wang, K. H. Low, *Numerical studies on modeling the near- and far-field wake vortex of a quadrotor in forward flight*, P. I. Mech. Eng. G-J. Aer. **236**(6) (2022), 1166–1183.
6. Y.-J. Go, J.-H. Bae, J. Ryi, J.-S. Choi, C.-R. Lee, *A study on the scale effect according to the Reynolds number in propeller flow analysis and a model experiment*, Aerospace **9**(10) (2022), 559.
7. C. Russell, G. Willink, C. Theodore, J. Jung, B. Glasner, *Wind tunnel and hover performance test results for multicopter UAS vehicles*, NASA/TM-2018-219758, NASA Ames Research Center, Moffett Field, CA, 2018.
8. A. Kovačević, J. Svorcan, M. S. Hasan, T. Ivanov, M. Jovanović, *Optimal propeller blade design, computation, manufacturing and experimental testing*, Aircr. Eng. Aerosp. Tec. **93**(8) (2021), 1323–1332.
9. J. Svorcan, K. Wang, C. Ivey, A. Kovačević, *Estimating the performance of a small-scale non-isolated propeller in hover using WMLES*, in: P. Moin, K. Maeda (eds.), *Annual Research Briefs* **2022**, 87–95, Center for Turbulence Research, Stanford, 2022.
10. P. Moin, J. Bodart, S. Bose, G. I. Park, *Wall-modeling in complex turbulent flows*, Note. N. Fl. Mech. Mul. D. **133** (2016), 207–219.
11. T. Mukha, S. Rezaeiravesh, M. Liefvendahl, *A library for wall-modelled large-eddy simulation based on OpenFOAM technology*, Comput. Phys. Commun. **239** (2019), 204–224.
12. C. Schwarz, A. Bodling, C. C. Wolf, R. Brinkema, M. Potsdam, A. D. Gardner, *Development of secondary vortex structures in rotor wakes*, Exp. Fluids **63**(1) (2022), 4.
13. J. N. Abras, R. Narducci, N. Hariharan, *Impact of high-fidelity simulation variations on wake breakdown of a rotor in hover*, AIAA 2020-0531, AIAA SciTech 2020 Forum, 2020.
14. I. Kostić, *Some practical issues in the computational design of airfoils for the helicopter main rotor blades*, Theor. Appl. Mech. (Belgrade) **31**(3–4) (2004), 281–315.
15. A. W. Vreman, *An eddy-viscosity subgrid-scale model for turbulent shear flow: Algebraic theory and applications*, Phys. Fluids **16** (2004), 3670–3681.
16. S. Kawai, J. Larsson, *Wall-modeling in large eddy simulation: Length scales, grid resolution, and accuracy*, Phys. Fluids **24** (2012), 015105.
17. Đ. Čantrak, N. Janković, D. Ilić, *Investigation of the turbulent swirl flow in pipe generated by axial fans using PIV and LDA methods*, Theor. Appl. Mech. (Belgrade) **42**(3) (2015), 211–222.

СИМУЛАЦИЈА ВЕЛИКИХ ВРТЛОГА ОКО МАЛИХ ЕЛИСА ПОМОЋУ WMLES МЕТОДЕ – ПРОЦЕНА АЕРОДИНАМИЧКИХ ПЕРФОРМАНСИ И ВИЗУЕЛИЗАЦИЈА ВРТЛОЖНОГ ТРАГА

Резиме. Зидно моделована симулација великих вртлога (енг. WMLES) је напредни математички модел турбулентних струјања којим се изналази филтрирано нумеричко решење. Додатни (енг. SGS) модел се користи за урачунавање ефеката неразрешених малих турбулентних структура на веће разрешене (т.j. за дисипацију на мањим размерама), док се понашање флуида у близини зидова моделира зидним функцијама (чиме се смањују захтеви за финоћом/квалитетом прорачунске мреже). Овај рад испитује могућности примене овог модела при процени аеродинамичких перформанси малих елиса, као и при анализи вртложног трага који се формира ниструјно. Индукована струјна поља око два пропелера пројектована за беспилотне летелице (приближних пречника 25 cm и 75 cm) у лебдењу су посматрана као нестационарна и турбулентна (нестишљива или стишљива, редом). Потешкоће прорачуна ових струјања углавном потичу од ниских вредности Рејнолдсовог броја (од неколико десетина до неколико стотина хиљада) када прелазно струјање и други струјни феномени могу бити присутни. Избор нумеричког модела потврђен је поређењем нумеричких са доступним експерименталним подацима. Док је глобалне карактеристике, као што су вучна сила и потребна снага (и њихови коефицијенти), могуће проценити са задовољавајућом тачношћу (до неколико процената), уочавање доминантних струјних одлика и даље представља изазов (и захтева додатне прорачунске напоре). Овде су вртложни трагови који се формирају иза ротора елиса илустровани и анализирани. Ова два референтна примера пружају корисне смернице за даље нумеричке и експерименталне студије малих пропелера.

Department of Aerospace Engineering
Faculty of Mechanical Engineering
University of Belgrade
Belgrade
Serbia
jsvorcan@mas.bg.ac.rs

(Received 12.10.2023)
(Revised 14.11.2023)
(Available online 13.12.2023)